Available online at www.sciencedirect.com
SCIENCE DIRECT®
ELSEVIER
Journal of Chromatography A, 984 (2003) 173–183
JOURNAL OF CHROMATOGRAPHY A
www.elsevier.com/locate/chroma

On-line solid-phase extraction of ceramides from yeast with ceramide III imprinted monolith

Minlian Zhang[a], Jianping Xie[a], Quan Zhou[b], Guoqiang Chen[b], Zheng Liu[a,*]
[a]*Department of Chemical Engineering, Tsinghua University, Beijing 100084, China*
[b]*Department of Biological Science and Biotechnology, Tsinghua University, Beijing 100084, China*

Received 29 July 2002; received in revised form 4 November 2002; accepted 6 November 2002

Abstract

A molecularly imprinted polymeric monolith (MIPM) was prepared by in situ polymerization using styrene, glycidyl methacrylate and methacrylic acid as monomers, divinylbenzene and triallyl isocyanurate as cross-linking agents, and ceramide III as print molecule. The texture, pore size distribution, mobile phase flow characteristic, and chromatographic performance of the MIPM and a control monolith synthesized without the print molecule were examined, respectively. The results showed that using ceramide III as print molecule significantly affected the pore structure and pore distribution of the monolith, and greatly improved the retention of ceramide III and its analogues used in cosmetics as well. The retention of ceramide III on the MIPM could be reduced by increasing the ratio of chloroform to hexane in eluting buffer. The workability of the MIPM was firstly demonstrated through the separation of a model lipid mixture containing ceramide III and ergosterol, the main sterol impurity in yeast lipid extracts. The application of the ceramide III imprinted monolith to the isolation of ceramides from yeast lipid extracts was attempted and resulted in a considerable enrichment of ceramides, as shown by FTIR analysis. This indicates the potential of ceramide III imprinted monolith synthesized in the present study in the on-line solid-phase extraction of ceramides from yeast.

Keywords: Stationary phases, LC; Monolithic columns; Solid-phase extraction; Ceramides; Molecularly imprinted polymers

1. Introduction

Chromatography using molecularly imprinted media has attracted growing attention due to its potential high selectivity contributed by the matrixes prepared with a chosen target molecule as template. Wulff et al. first synthesized imprinted polymers by means of free radical copolymerization, in which a complex between monomers and imprint molecule was formed via reversible covalent bonds before polymerization. After polymerization, cavities with size, shape and chemical functionality complementary to that of the template molecule could be created [1,2]. Later, Mosbach et al. developed a non-covalent imprinting approach that was more flexible concerning the choice of functional monomers, target molecules and the use of the imprinted materials [3]. Since then a great number of studies have been attempted by using a wide range of compounds as print molecules, and this approach appeared par-

*Corresponding author. Tel.: +86-10-6277-9876; fax: +86-10-6277-0304.
E-mail address: liuzheng@tsinghua.edu.cn (Z. Liu).

0021-9673/02/$ – see front matter
PII: S0021-9673(02)01847-2

ticularly effective in the enrichment and purification of small molecules [4–10].

Ceramide is an amide of fatty acid with hydroxylated long chain amine, as shown in Fig. 1. The fatty acids and the long chain bases vary in length, degree of unsaturation or hydroxylation and thus give rise to a group of molecules called ceramides [11]. Ceramides play an important role as the main structural lipids of skin, hair and nails of humans and animals, functioning as an effective barrier to the loss of water, and to the physical, chemical or biological influences from the environment [12,13], leading to a rapidly growing application of ceramides to cosmetics [14]. Moreover, recent studies revealed the function of ceramides as important second messages for various cellular processes, such as apoptosis, cell cycle arrest, cell differentiation, cell propagation, and induction of cytokine synthesis [15–19], as well as its capacity to inhibit carcinogenesis [20]. There appears to be a great potential for ceramides as pharmaceuticals.

To date, ceramides used in cosmetics are mainly extracted from natural resources such as skin of humans and animals, blood cells, bovine brain, egg, plants and yeast [21,22]. The advantages in terms of being non-toxic and amenable to genetic manipulation make yeast particularly suitable for large-scale production of ceramides [21]. However, the separation and purification of ceramides from yeast are challenged by the structural diversity, low content, i.e. less than 1% of overall lipids in yeast, and lack of chromophores [11]. At this moment, preparative thin-layer chromatography is the most effective method for ceramide purification [23–25]. Unfortunately, this method is tedious, time-consuming, sensitive to sample loading and thus not suitable for large-scale separation. The development of an effective method for large-scale separation of ceramides is

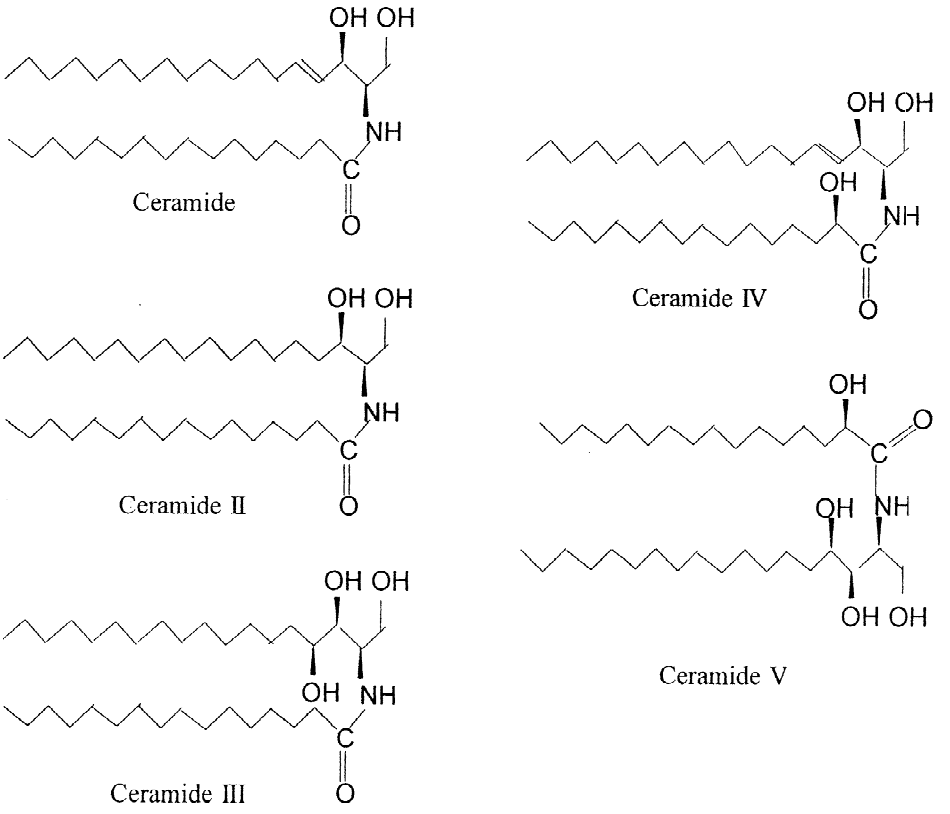

Fig. 1. Structure of ceramides.

thus of essential importance for the potential application of ceramides, as described above.

The number and nature of functional groups in ceramides seemed to be suitable to design specific recognition cavities with the non-covalent approach. Thus we directed our attention to applying molecular imprinting technology to ceramide enrichment. In general, the molecularly imprinted chromatographic media are particles obtained by grinding and sieving bulk polymers. Matsui et al. simplified the preparation procedure with employing an in-situ polymerization technique developed by Svec and Frechet [26,27]. In the present study, we developed a ceramide imprinted polymeric monolith made by in-situ polymerization. Based on the previous study [28], styrene, glycidyl methacrylate and methacrylic acid were chosen as monomers, divinylbenzene and triallyl isocyanurate as cross-linking agents and ceramide III as print molecule. The variations of texture and pore size distribution due to the addition of the template were examined by scanning electron micrography and mercury porosimetry, and subjected to a comparison with a control monolith prepared without the print molecule. The chromatographic behavior of the MIPM in terms of liquid flow resistance, retention of ceramide species, as well as the separation performance, was examined, respectively, using chloroform–hexane as mobile phase and evaporative light scattering detection (ELSD) as detector. Finally, the application of ceramide III imprinted monolith to the enrichment of ceramides from yeast lipids was attempted and the concentrated ceramides were analyzed by Fourier transform infrared (FTIR).

2. Materials and methods

2.1. Materials

Glycidyl methacrylate (GMA) (97%), methacrylic acid (MAA) and triallyl isocyanurate (TAIC) were purchased from Acros Organics (Geel, Belgium) and used without further purification. Styrene (ST) and divinylbenzene (DVB) (56% divinyl monomer) obtained from Alfa Aesar (Ward Hill, MA, USA) were extracted with 10% aqueous sodium hydroxide and water, dried over anhydrous magnesium sulfate, and distilled under vacuum. 2,2′-Azobis-(isobutyronitrile) (AIBN) was obtained from Tianjin Dagu Chemical Plant (Tianjin, China) and recrystallized in ethanol before use. Ceramides II, III and V were generously provided by Procter & Gamble (Cincinnati, USA) and ceramide IV was purchased from Sigma (St. Louis, MO, USA). The previous results showed that ceramide III was the major ceramide component in the yeast strain studied in this project [29]. Thus we selected ceramide III as the print molecule. The FTIR spectrum of ceramide III used in the present study is shown in Fig. 2. The yeast used in the present study was purchased from Hubei Angel Yeast (Hubei, China). Other reagents were all

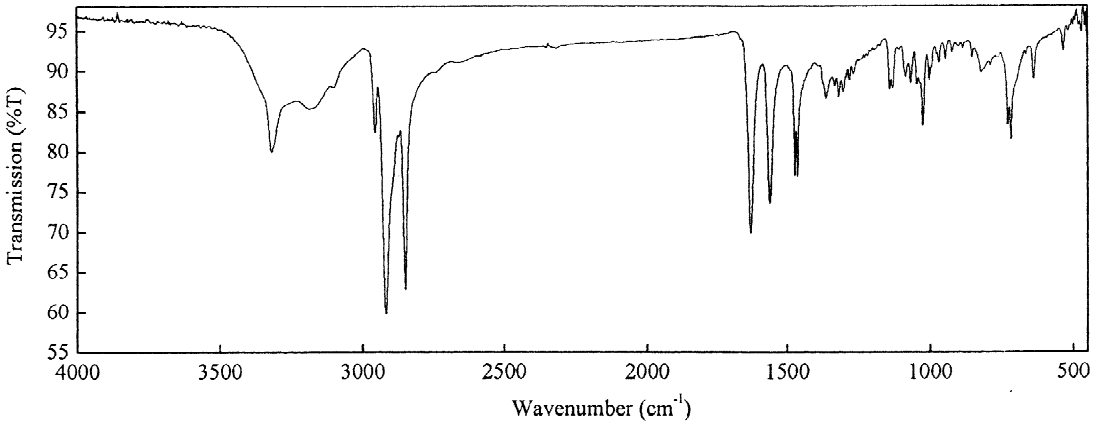

Fig. 2. FTIR spectrum of ceramide III provided by P&G.

of analytical grade and delivered from standard suppliers.

2.2. Preparation of the MIPM and the control monolith

One ml of monomers (GMA, MAA and ST, 2:3:5, mol/mol), 0.5 ml of cross-linking agents (DVB and TAIC, 2:1, mol/mol), 1.5 ml of porogenic agents (toluene and heptane, 1.8:1, w/w), AIBN (2 mol.% with respect to monomers) and 20 mg of ceramide III were poured into a stainless steel tube of 150×4.6 mm I.D. sealed at one end and degassed in an ultrasonicator for 15 min. Then the other end was sealed and the polymerization was allowed to proceed at 65 °C for 4 h, 75 °C for 4 h and finally 85 °C for 4 h. After this polymerization, the seals at the two ends of the tube were removed. The column was attached to a HP HPLC system, as described below, and washed to remove the porogenic agents and the template molecule with 200 ml of ethanol. The control monolith was also prepared using the same reaction mixture but without the template molecule, ceramide III.

2.3. Characterization of the MIPM and the control monolith

The monolith was taken out of the tube after the chromatographic experiments, cut into small pieces, and dried at 70 °C for 24 h. The pore structure of the monolith was characterized by scanning electron microscopy (SEM) carried out in a KYKY 2000 (Beijing ZHONGKE KEYI Technology Development, China). All samples were sputter-coated with gold before SEM assay. The pore size distribution was determined by mercury porosimetry with an Autoscan-33 porosimeter (Quanta, USA).

2.4. Extraction of lipids

Lipids were extracted from the yeast by a modified procedure described by Itoh and Kaneko [30]. Five grams of dry yeast cells were suspended in 50 ml of chloroform–methanol (1:2, v/v) and stirred for 5 h at room temperature. The suspension was filtered through a glass-sintered filter, and the residual cells were washed with 50 ml of chloroform–methanol (1:2, v/v). The extract was evaporated under a stream of nitrogen gas, resuspended in an appropriate volume of chloroform, and stored at −10 °C.

2.5. Assay

HPLC analysis was performed with a HP 1100 HPLC system (Hewlett-Packard, USA), consisting of a quaternary pump, a vacuum degasser, a thermostatted column compartment, a 20-μl manual injector and a HP Chemstation for data analysis. Detection was carried out using an Alltech 500 evaporative light scattering detector by Alltech Associates (Deerfield, USA) where the drift tube temperature was set at 60 °C and the flow-rate of the nebulizer gas, nitrogen, at 2.0 l/min (linear flow-rate). The total void volume including precolumn, column and postcolumn was determined by the injection of acetone with methanol as mobile phase and UV as detector.

2.6. FTIR analysis

FTIR spectra were obtained with a Perkin-Elmer spectrometer (USA) with a scanning range from 4000 to 450 cm^{-1} and a resolution of 2 cm^{-1}. The sample for FTIR experiment was prepared by dropping its solution on a KBr pellet and evaporating the solvent.

3. Results and discussion

3.1. Characterization of the monoliths

Aimed at application, much of the research into molecularly imprinted polymers is focused on the change of retention behavior of the matrix before and after molecular imprinting [31–34]. The variations of polymer texture, pore size distribution and flow characteristics produced by molecular imprinting, however, have not yet been paid adequate attention, though they are fundamental to elucidate the retention mechanism.

The SEM graphs of the MIPM and the control monolith are shown in Fig. 3. Compared to the control monolith that is characterized by large pores of the order of several microns formed by continuous three-dimensional clusters of fused microspheres of

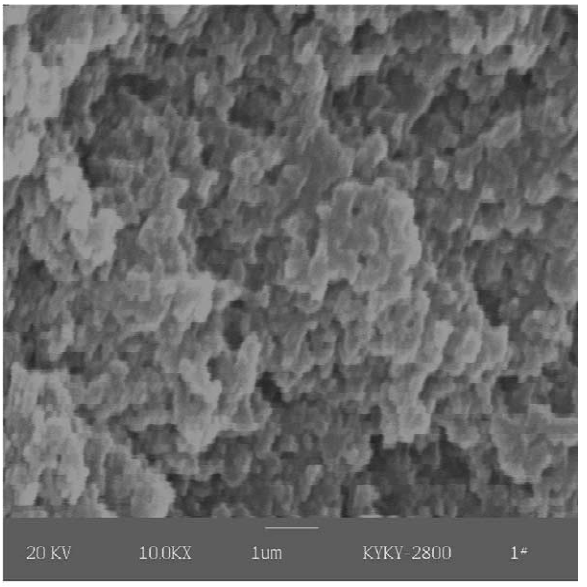

(A)

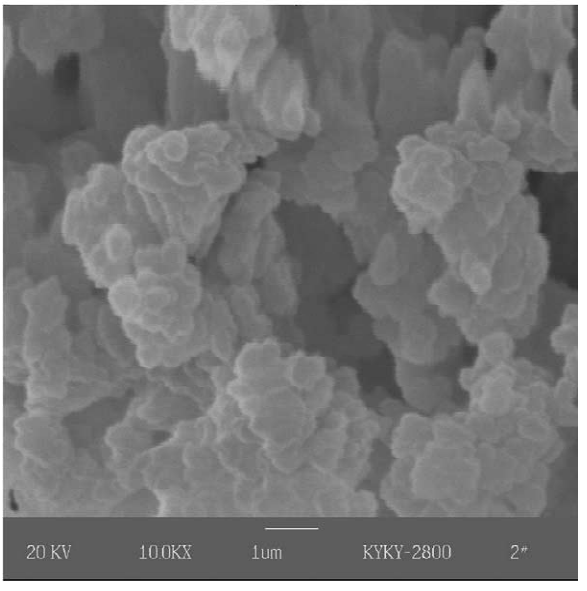

(B)

Fig. 3. Scanning electron micrographs of the MIPM (A) and the control monolith with magnifications of 10,000.

400 to 1000 nm, the MIPM presents smaller pores of the order of less than 1 μm in diameter. The other major difference between the MIPM and the control monolith is their skeletons, in which the typical clusters made by microspheres, as shown by the control monolith, did not appear in the MIPM.

The presence of porogenic agents (precipitators) during the polymerization can greatly effect the solubility of the polymer molecules in the polymerization system, as described elsewhere [35–37], and resulted in matrices with different structures in terms of pore structure, pore size distribution, and porosity. Similar function was identified for ceramide III, as shown by Fig. 3. Ceramide is an amphiphatic molecule with hydrophobic long carbon chains and hydrophilic amide and hydroxyl groups, which may enhance the solubilization of the copolymer in the porogenic agents, retard phase separation, and promote the formation of large aggregates. It should be noted that the sample preparation for SEM, e.g. drying and cutting, may also lead to additional changes in the structures of the MIPM and the control monolith. In this case, the measured pore size may be different from the original sample, as described elsewhere [38].

Fig. 4 shows the pore size distribution determined via mercury porosimetry. Here the control monolith has a pore size distribution from 150 to 5000 nm with a distinct maximum near 2200 nm. In contrast, the MIPM consists of pores with size ranging from 100 to 600 nm with a distinct maximum near 300

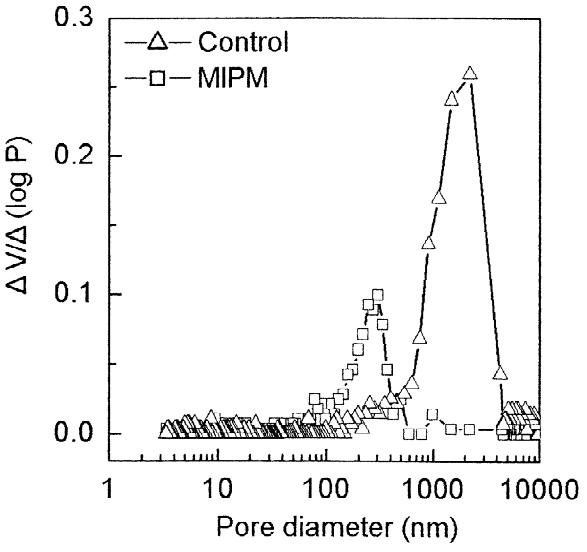

Fig. 4. Pore size distribution curves measured with mercury intrusion porosimetry.

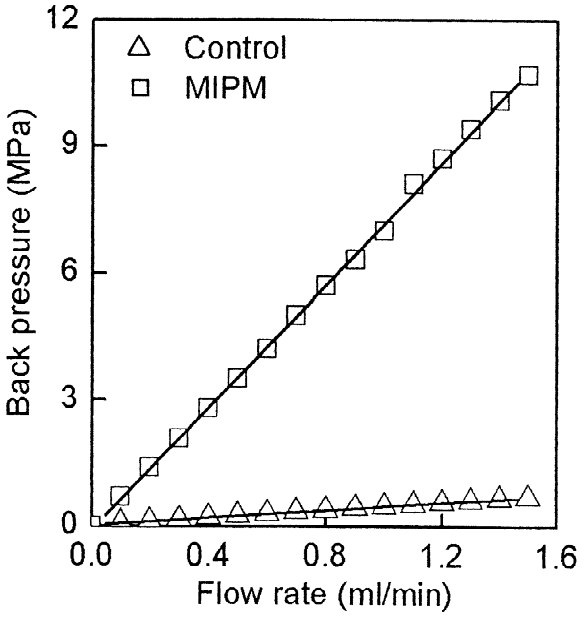

Fig. 5. Back pressure as a function of mobile phase flow velocity in the control and the MIPM column with hexane as mobile phase.

nm. These results are in good agreement with those obtained by SEM, as shown by Fig. 3.

Fig. 5 shows the back-pressure of the MIPM and the control monolith prepared by in-situ polymerization as a function of flow-rate. Here the MIPM shows a much higher back-pressure over the control monolith. This difference may be mainly attributed to the different pore structures of the MIPM and the control, as shown by Fig. 3. Though the porosity of these two columns are not being accurately determined, it could be concluded from the chromatographic results that the MIPM and the control monolith possess a similar porosity, as indicated by their similar void volume. It is also shown by Fig. 5 that within the operating pressure up to 10.0 MPa, a linearity of the back-pressure versus flow velocity is achieved, indicating that the MIPM is stable and not compressed.

3.2. Retention of the print molecule on the MIPM and the control monolith

The effectiveness of the imprinting process can be shown by the retention of the print molecule on the MIPM and the control monolith. The void volumes of the control and the imprinted monolith detected with acetone as marker were 2.62 and 2.68 ml, respectively. The elution curves of ceramide III on the control and the MIPM are shown in Fig. 6. On the control monolith, the retention volume of ceramide III is almost identical to that of the void volume. In contrast, a significant increase in the retention volume is obtained on the MIPM, indicating a successful imprinting of ceramide III. Due to the presence of methacrylic acid functionality, the control monolith may interact with the template via hydrogen bonding or/and ionic interaction [39,40]. The result in Fig. 6 also shows that the non-specific interaction between the monolith support and ceramide III is very weak and does not lead to additional retardations of ceramide III.

The elution curves of ceramide III on the MIPM with different ratios of chloroform to hexane in the mobile phase are shown in Fig. 7, in which the increase of the ratio of chloroform to hexane leads to a corresponding reduction of the retention time of ceramide III. It is known that the template molecule

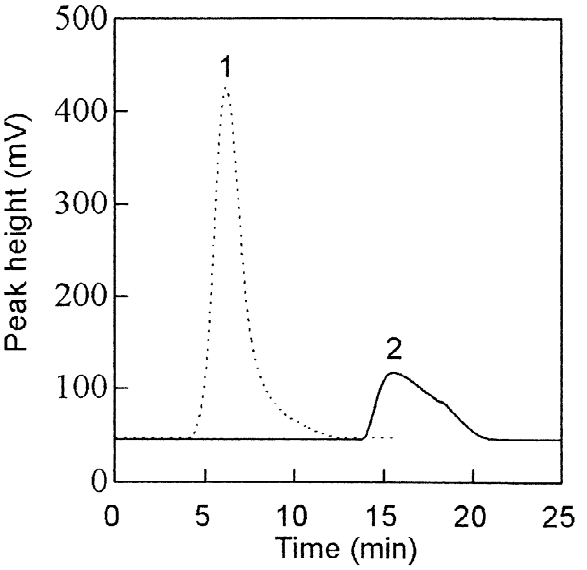

Fig. 6. Chromatograms of ceramide III on the control column (1) and the MIPM column (2). Conditions: mobile phase for the control monolith, chloroform–hexane 20:80 and for the MIPM column, gradient produced with chloroform and hexane, 30:70 chloroform–hexane in 5 min, 30:70–50:50 chloroform–hexane in 5 min; flow-rate, 0.5 ml/min; injection volume, 20 μl; concentrations, 1 mg/ml in chloroform.

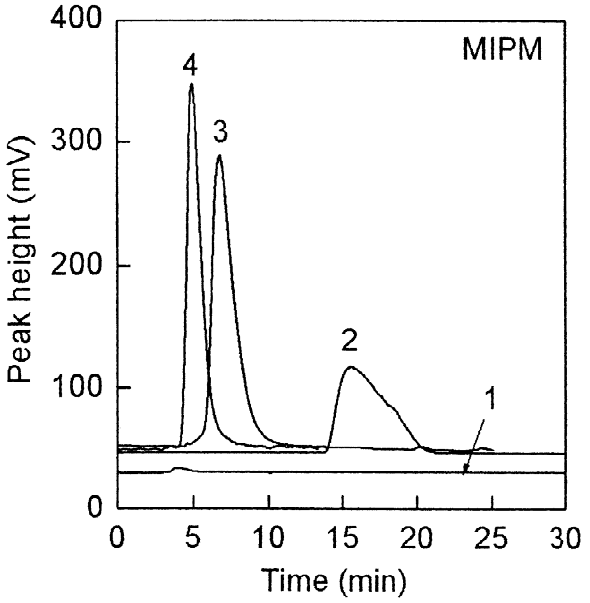

Fig. 7. Elution of ceramide III on the MIPM column with different ratios of chloroform to hexane, 20:80 (1), gradient 30:70 in 5 min, 30:70–50:50 in 5 min (2), 50:50 (3) and 100:0 (4). Conditions: flow velocity, 0.5 ml/min; injection volume, 20 μl; concentration, 1 mg/ml in chloroform.

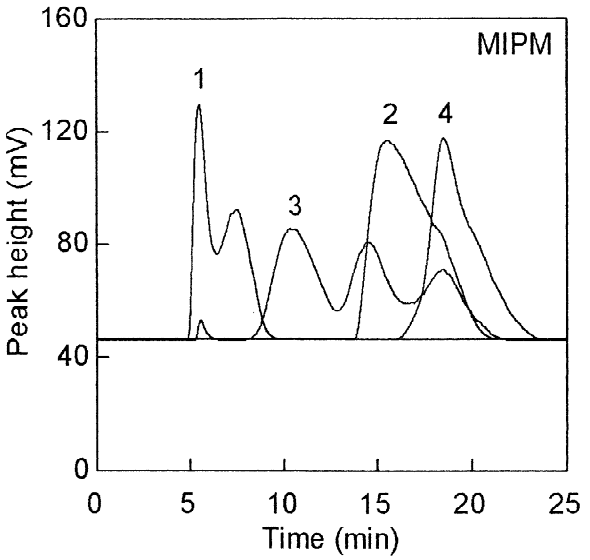

Fig. 8. Elution of ceramides II (1), III (2), IV (3) and V (4) on the MIPM column. Conditions: mobile phase gradient 30:70 chloroform–hexane in 5 min, 30:70–50:50 chloroform–hexane in 5 min; flow velocity, 0.5 ml/min; injection volume, 20 μl; ceramide concentrations, 1 mg/ml in chloroform.

can interact with its molecularly imprinted polymer via hydrogen bonding, ionic, π–π and/or hydrophobic interactions [41]. Ceramides possess hydroxyl groups, amide and long carbon chains, and can thus interact with the imprinted poly(GMA–MAA–ST–DVB–TAIC) via hydrophobic, hydrogen bonding and ionic interactions. Reduction of the retention time of ceramide III, as a result of increasing the ratio of chloroform to hexane in eluent, indicated that polar interactions, such as hydrogen bonding were probably the major interactions between MIPM and ceramide III, the template.

Concerning the diversity of ceramides extracted from yeast, which may be valuable cosmetic additives, we also examined the adsorption capability of the MIPM to ceramide analogues. None of ceramides II, III, IV and V can be eluted within 30 min with a mobile phase composition of chloroform–hexane 20:80. Gradient elution of the ceramides from the MIPM was then attempted by increasing the ratio of chloroform to hexane. The results shown in Fig. 8 indicate an elution sequence, i.e. ceramides II, IV, III, V, in the MIPM. This is different from the results obtained in the reversed-phase or normal-phase mode [42–46], indicating a different retention mechanism. It is also worthy of noting that ceramide IV from Sigma is a mixture of various ceramide structures, therefore its elution is presented by four peaks around the ceramide III peak. Meanwhile, the MIPM imprinted with ceramide III possesses the highest retention to ceramide V rather than the print molecule.

Fig. 9 shows the retention of the above ceramide species on the control monolith. No retardation is obtained for ceramides II, III and IV in case of using chloroform–hexane 20:80 as mobile phase. However, ceramide V was not eluted within 30 min, indicating the occurrence of strong interaction between ceramide V and the control monolith. Line 5 in Fig. 9 was the elution curve of ceramide V using the identical gradient elution described above.

3.3. Separation of ceramide III and ergosterol with ceramide III imprinted monolith

In order to examine the workability of the MIPM to enrich ceramides from yeast extracts, we firstly

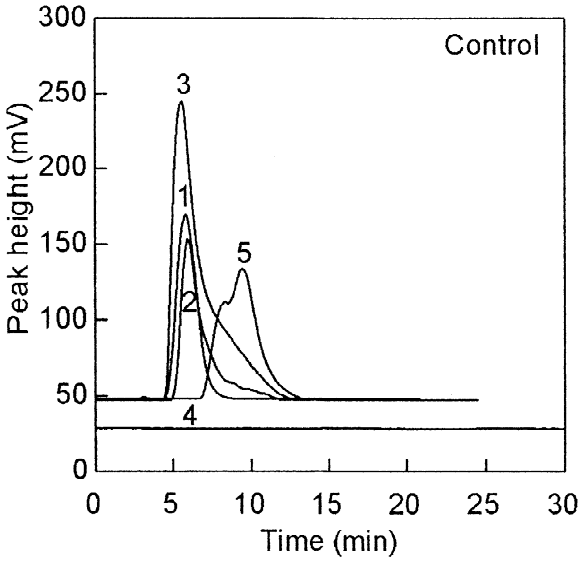

Fig. 9. Elution of ceramides II, III, IV and V on the control monolith. Conditions: mobile phase 20:80 chloroform–hexane for ceramides II (1), III (2), IV (3) and V (4), gradient 30:70 chloroform–hexane in 5 min, 30:70–50:50 chloroform–hexane in 5 min for ceramide V (5); flow velocity, 0.5 ml/min; injection volume, 20 μl; ceramide concentrations, 1 mg/ml in chloroform.

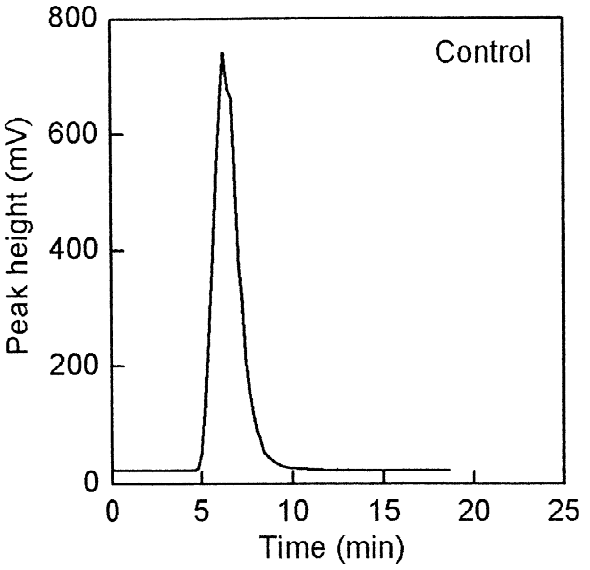

Fig. 10. Separation of ceramides III and ergosterol on the control monolith. Conditions: mobile phase gradient 30:70 chloroform–hexane in 5 min, 30:70–50:50 chloroform–hexane in 5 min; flow velocity, 0.5 ml/min; injection volume, 20 μl; sample concentrations, 1 mg/ml in chloroform.

applied it to the separation of a model lipid mixture consisting of ceramide III and ergosterol, the major sterol in yeast lipids [47]. Again, the separation was performed on control and the MIPM, respectively. Fig. 10 shows that ceramide III and ergosterol were both excluded from the control monolith within the void volume. The MIPM shows a selective retention to ceramide III, as shown by Fig. 11.

3.4. On-line solid-phase extraction of ceramides from yeast

On-line solid-phase extraction of ceramides from yeast extract by adsorption on MIPM is shown in Fig. 12. According to the elution experiments described above, the elution was firstly performed using an eluent of chloroform–hexane 20:80 in order to remove bulk yeast lipids. Then an eluent of chloroform–hexane 50:50 was applied to elute ceramides from the MIPM and subjected to purity analysis by FTIR.

The FTIR spectra of the yeast lipids and the enriched ceramides are shown in Figs. 13 and 14,

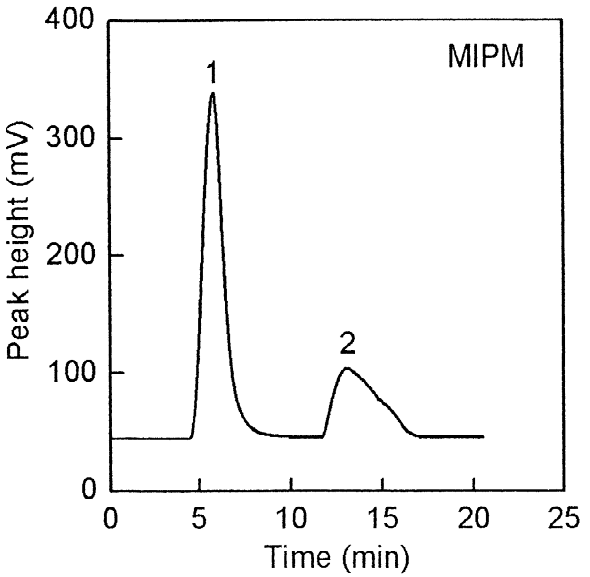

Fig. 11. Separation of ergosterol (1) and ceramides III (2) on the MIPM column. Conditions: mobile phase gradient 30:70 chloroform–hexane in 5 min, 30:70–50:50 chloroform–hexane in 5 min; flow velocity, 0.5 ml/min; injection volume, 20 μl; sample concentrations, 1 mg/ml in chloroform.

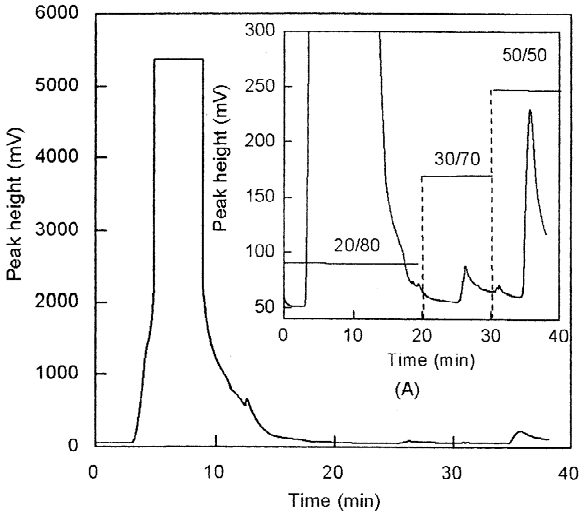

Fig. 12. Recovery of ceramides from yeast lipids on the MIPM column. Conditions: mobile phase gradient 20:80 chloroform–hexane in 20 min, 30:70 chloroform–hexane in 10 min, 50:50 chloroform–hexane in 20 min; flow velocity, 0.5 ml/min; injection volume, 100 μl. (A) is part of the eluent curve.

respectively. Compared to Fig. 13, a distinct peak at 1633 cm^{-1}, the typical peak for ceramides [48,49], appears in the FTIR spectrum of the enriched fraction shown in Fig. 14. This can be attributed to the selective adsorption of ceramides on the MIPM

For the present study, the MIPM was used for 6 months and no obvious changes in back-pressure, retention behavior, and adsorption properties were observed with the number of injections. The results show that the MIPM is stable and can withstand long-term use for ceramide enrichment from yeast lipids.

4. Conclusion

The extra low content and the structure diversity make ceramides a challenging model for molecular imprinting technology. The present study started with in situ synthesis of ceramide III imprinted monolith (MIPM). Then the texture, pore size distribution, as well as the retention behavior of the MIPM were examined and subjected to a comparison to a control monolith. It is shown that the addition of the template, ceramide III, into the reaction mixture resulted in a remarkably different structure characterized by small pore size, high back-pressure and effective retention of the template molecule. Nonspecific adsorption of ceramide III, the template, on the solid matrix of the control monolith was not observed. Gradient elution of ceramides from MIPM indicated the polar interaction is the major interaction between the ceramides and the MIPM. Finally, separation of ceramide III from ergosterol and recovery of ceramides from yeast extract were attempted. The successful recovery of ceramides from yeast, as shown by FTIR analysis, indicated the potential of the MIPM in the on-line solid-phase extraction of ceramides from yeast extracts. Application of the MIPM to the separation and purification of ceramides will also be attempted.

It is interesting to note the distinctly different structures of the MIPM and the control monolith,

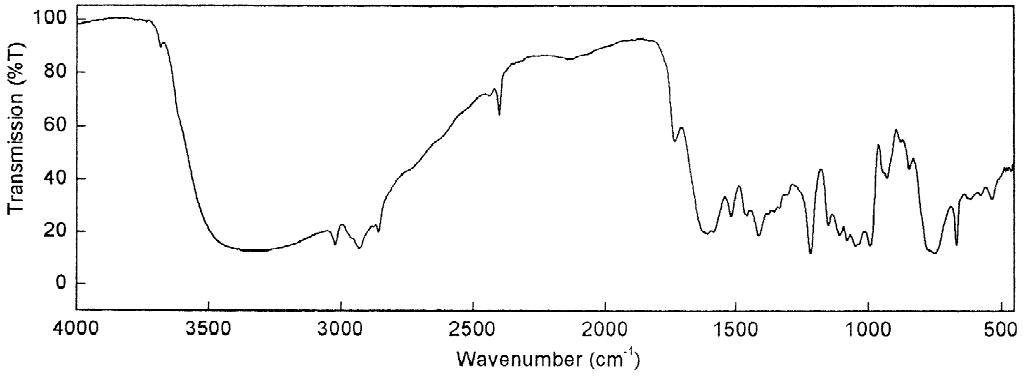

Fig. 13. FTIR spectrum of the yeast lipid extract.

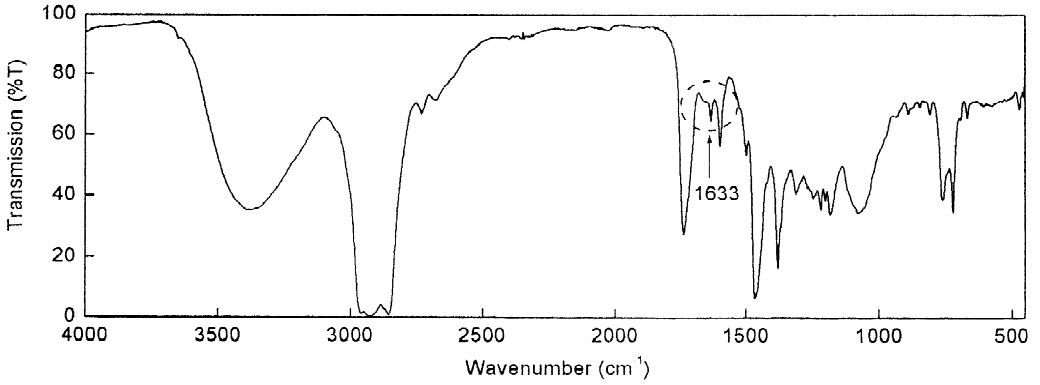

Fig. 14. FTIR spectrum of the ceramides fraction from yeast.

resulting from the addition of the template, ceramide III. This will lead our attention into the function of the template during the polymerization of the MIPM. Also, within the scope of our further study is the interaction between the template and the monolith, which will provide a basis for the development of ceramide imprinted monoliths with high-performance in terms of high selectivity and high capacity.

Acknowledgements

The work was supported by THSJZ and the National Natural Science Foundation, PR China under project numbers 29876020, 20176023 and 20206013.

References

[1] G. Wulff, A. Sarhan, Angew. Chem. Int. Ed. 11 (1972) 341.
[2] G. Wulff, Angew. Chem. Int. Ed. 34 (1995) 1812.
[3] K. Mosbach, Trends Biochem. Sci. 19 (1994) 9.
[4] R.F. Venn, R.J. Goody, Chromatographia 50 (1999) 407.
[5] J.C. Xie, L.L. Zhu, H.P. Luo, L. Zhou, C.X. Li, X.J. Xu, J. Chromatogr. A 934 (2001) 1.
[6] K. Ensing, C. Berggren, R.E. Majors, LC–GC Eur. 15 (2002) 16.
[7] B. Bjarnason, L. Chimuka, O. Ramstrom, Anal. Chem. 71 (1999) 2152.
[8] I. Ferrer, F. Lanza, A. Tolokan, V. Horvath, B. Sellergren, G. Horvai, D. Barcelo, Anal. Chem. 72 (2000) 3934.
[9] R. Koeber, C. Fleischer, F. Lanza, K.S. Boos, B. Sellergren, D. Barcelo, Anal. Chem. 73 (2001) 2437.
[10] J.D. Lei, T.W. Tan, Acta Chim. Sin. 60 (2002) 1279.
[11] A.E. Cremesti, A.S. Fischl, Lipids 35 (2000) 937.
[12] D.T. Downing, M.E. Stewart, P.W. Wertz, J. Invest. Dermatol. 88 (1987) 2s.
[13] K. Raith, R.H.H. Neubert, Anal. Chim. Acta 403 (2000) 295.
[14] K.D. Paepe, D. Roseeuw, V. Rogiers, Cosmet. World J. 798 (1998) 1.
[15] J.D. Fishbein, R.T. Dobrowsky, A. Bielawska, S. Garrett, Y.A. Hannun, J. Biol. Chem. 268 (1993) 9255.
[16] L.M. Obeid, Y.A. Hannun, J. Cell Biochem. 58 (1995) 191.
[17] T. Okazaki, T. Kondo, T. Kitano, M. Tashima, Cell Signal. 10 (1998) 685.
[18] J. Pfeilschifter, A. Huwiler, News Physiol. Sci. 15 (2000) 11.
[19] M.R. Lopez, G. Gutierrez, C. Mendoza, J.L. Ventura, L. Sanchez, E.R. Maldonado, A. Zentella, L.F. Montano, Biochem. Biophys. Res. Commun. 293 (2002) 1028.
[20] Y.A. Hannun, Science 274 (1996) 1855.
[21] J. Rupcic, V. Maric, Chem. Phys. Lipids 91 (1998) 153.
[22] M. Philip, B. Rupee, D. Symolia, Chinese Patent Application 96101950.
[23] F. Bonte, P. Pinguet, J.M. Chevalier, A. Meybeck, J. Chromatogr. B 664 (1995) 311.
[24] S. Zellmer, J. Lasch, J. Chromatogr. B 691 (1997) 321.
[25] J. Bodennec, G. Brichon, O. Koul, M.I. Babili, G. Zwingelstein, J. Lipid Res. 38 (1997) 1702.
[26] F. Svec, J.M.J. Frechet, Science 273 (1996) 205.
[27] J. Matsui, T. Kato, T. Takeuchi, M. Suzuki, K. Yokoyama, E. Tamiya, I. Karube, Anal. Chem. 65 (1993) 2223.
[28] M.L. Zhang, Y. Sun, J. Chromatogr. A 912 (2001) 31.
[29] J. Rupcic, C. Milin, V. Maric, Syst. Appl. Microbiol. 22 (1999) 486.
[30] T. Itoh, H. Kaneko, Yukagaku 23 (1974) 350.
[31] B. Sellergren, J. Chromatogr. A 673 (1994) 133.
[32] J. Haginaka, H. Takekira, K. Hosoya, N. Tanaka, J. Chromatogr. A 849 (1999) 331.
[33] M.C. Hennion, J. Chromatogr. A 856 (1999) 3.
[34] A. Ellwanger, P.K. Owens, L. Karlsson, S. Bayoudh, P. Cormack, D. Sherrington, B. Sellergren, J. Chromatogr. A 897 (2000) 317.
[35] W.L. Sederel, G.J. De Jong, J. Appl. Polym. Sci. 17 (1973) 2835.

[36] H. Jacobelli, M. Bartholin, A. Guyot, J. Appl. Polym. Sci. 23 (1979) 927.
[37] F. Svec, J.M.J. Frechet, Macromolecules 28 (1995) 7580.
[38] J.L. Liao, R. Zhang, S. Hjerten, J. Chromatogr. 586 (1991) 21.
[39] C.C. Hwang, W.C. Lee, J. Chromatogr. B 765 (2001) 45.
[40] C. Yu, K. Mosbach, J. Org. Chem. 62 (1997) 4057.
[41] O. Ramstrom, R.J. Ansell, Chirality 10 (1998) 195.
[42] J.Y. Zhou, P. Chaminade, K. Gaudin, P. Prognon, A. Baillet, D. Ferrier, J. Chromatogr. A 859 (1999) 99.
[43] K. Gaudin, P. Chaminade, D. Ferrier, A. Baillet, A. Tchapla, Chromatographia 49 (1999) 241.
[44] T. Gildenast, J. Lasch, Biochim. Biophys. Acta 1346 (1997) 69.
[45] M. Yano, E. Kishida, Y. Muneyuki, Y. Masuzawa, J. Lipid Res. 39 (1998) 2091.
[46] K.J. Robson, M.E. Stewart, S. Michelsen, N.D. Lazo, D.T. Downing, J. Lipid Res. 35 (1994) 2060.
[47] T. Nurminen, K. Konttinen, H. Suomalainen, Chem. Phys. Lipids 14 (1975) 15.
[48] R. Mendelsohn, D.J. Moore, Methods Enzymol. 312 (2000) 228.
[49] H.C. Chen, R. Mendelsohn, M.E. Rerek, D.J. Moore, Biochim. Biophys. Acta 1468 (2000) 293.